

# Numerical Modeling of Photodetectors Made from Two-Dimensional Materials

Ergun Simsek, Raonaqul Islam, and Curtis R. Menyuk

University of Maryland Baltimore County, Baltimore, MD, USA (simsek@umbc.edu)

**Abstract**—A concise numerical model, based on drift-diffusion equations and wave propagation in a multilayered medium, has been developed to investigate photodetectors composed of two-dimensional materials. Comparisons between the numerical results and experiments validate the precision of the proposed approach in calculating the quantum efficiency as a function of incident wavelength. The formulation also enables the calculation of advanced photodetector parameters such as phase noise and bandwidth.

## I. INTRODUCTION

Two-dimensional (2D) materials, particularly monolayers and a few layers of transition metal dichalcogenides (TMDs), have recently emerged as promising candidates for diverse optoelectronic applications [1]–[4]. Monolayer MoS<sub>2</sub>, for instance, exhibits unique properties, including a direct bandgap transformation upon transitioning from its bulk form, making it advantageous for applications such as transistors and optoelectronics [5], [6]. In contrast to graphene, MoS<sub>2</sub>'s direct bandgap allows for direct photon absorption and emission, enhancing its suitability for spintronics exploration. Various synthesis methods, such as chemical vapor deposition and liquid exfoliation, enable practical device fabrication [3].

Despite experimental advancements in photodetectors based on 2D materials such as monolayer of MoS<sub>2</sub>, there is a notable scarcity of numerical investigations characterizing the performance metrics of these devices; see [7] as an example. In this work, we introduce a compact yet accurate one-dimensional drift-diffusion framework [8] that takes wave propagation in multilayered media account to evaluate single-layer MoS<sub>2</sub> photodetectors, employing precise models to determine material properties [5], [6]. This approach, encompassing low-temperature photocarrier dynamics and layered media analysis, represents a unique contribution to the assessment of 2D material-based photodetectors.

## II. NUMERICAL MODEL

Figure 1 illustrates the design under consideration: a monolayer of MoS<sub>2</sub> is placed on top of a silicon-oxide-coated silicon substrate. The gates on the top function as source and drain contacts. The third contact is formed at the bottom for gating. The device is illuminated from the top, perpendicularly.

To calculate the carrier transport behavior, we solve for the drift-diffusion equations [8] that include the current continuity equations for both electrons and holes and the Poisson's equation, that are given by

$$\frac{\delta(n - N_D^+)}{\delta t} = G_L - R(n, p) + \frac{\nabla \cdot \mathbf{J}_n}{q}, \quad (1)$$

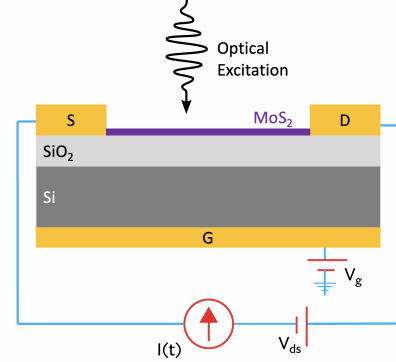


Fig. 1. Schematic illustration of the 2D material-based photodetector.

$$\frac{\delta(p - N_A^-)}{\delta t} = G_L - R(n, p) + \frac{\nabla \cdot \mathbf{J}_p}{q}, \quad (2)$$

$$\nabla \cdot \mathbf{E} = \frac{q}{\epsilon} (N_D^+ + p - n - N_A^-), \quad (3)$$

where,  $q$  is the charge of electron,  $G_L$  is generation rate of the MoS<sub>2</sub> layer,  $R$  is the recombination rate,  $\epsilon$  is the permittivity of MoS<sub>2</sub>, and  $N_D^+$  and  $N_A^-$  are the ionized donor and acceptor impurity concentrations.  $\mathbf{J}_n$  and  $\mathbf{J}_p$  are current densities for electrons and holes, which are determined with the drift-diffusion equations:

$$\mathbf{J}_n = qn\mathbf{v}_n(\mathbf{E}) + qD_n\nabla n, \quad (4)$$

$$\mathbf{J}_p = qp\mathbf{v}_p(\mathbf{E}) - qD_p\nabla p, \quad (5)$$

where,  $D_n$  and  $D_p$  are the electron and hole's diffusion coefficients,  $\mathbf{v}_n(\mathbf{E})$  and  $\mathbf{v}_p(\mathbf{E})$  are electric-field dependent electron and hole drift velocities, respectively.

To calculate the complex electrical permittivity of MoS<sub>2</sub> as a function of wavelength, temperature, and gating, we used the model described in [5]. The bandgap of monolayer MoS<sub>2</sub> is calculated using the Varshni equation,  $E_g(T) = E_g(0) - \alpha T^2 / ((T + \beta))$  [9], where,  $E_g(0) = 1.95$  eV,  $\alpha = 5.9 \times 10^{-4}$  eV/K, and  $\beta = 430$  K considered for our simulations. The other material parameters for monolayer MoS<sub>2</sub> are provided in Table I.

To evaluate the load resistance ( $R_{Load}$ ) of the device, we first calculate the sheet resistance,  $R_{sh} = 1/qn\mu(T)$ , of the MoS<sub>2</sub> monolayer, then use the obtained value to find  $R_{Load} = \sqrt{\rho_i \times R_{sh}}$  assuming  $\rho_i = 1/[(T - 100)/107]^3$  is the interfacial resistance between the contact and MoS<sub>2</sub>, with  $T$  being the temperature.

TABLE I  
MATERIAL PARAMETERS OF  $\text{MoS}_2$  AT  $T = 300\text{K}$  USED IN OUR SIMULATIONS.

Parameter Name	Symbol	Value
Energy bandgap at 300 K	$E_g$	1.87 eV
Electron's effective mass	$m_e^*$	0.35
Hole's effective mass	$m_h^*$	0.50
Electron affinity	$\chi_i$	4.27 eV
Radiative recombination coefficient	$B_r$	$10^{-7} \text{ cm}^3/\text{s}$
Auger coefficient	$C_n, C_p$	$10^{-24} \text{ cm}^6/\text{s}$
Density of states in conduction band	$N_C$	$3.76 \times 10^{11} \text{ cm}^{-2}$
Density of states in valence band	$N_V$	$5.76 \times 10^{11} \text{ cm}^{-2}$
Hole saturation velocity	$v_{p,\text{sat}}$	$4.2 \times 10^6 \text{ cm/s}$
Electron saturation velocity	$v_{n,\text{sat}}$	$1 \times 10^7 \text{ cm/s}$
Electron lifetime	$\tau_n$	$1 \times 10^{-9} \text{ s}$
Hole lifetime	$\tau_p$	$10 \times 10^{-9} \text{ s}$

The density of the induced carriers depends on the thickness and property of the oxide layer in between, i.e.,  $n_s = \epsilon_{\text{ox}}(V_g - V_{\text{th}})/t_{\text{ox}}$ , where  $\epsilon_{\text{ox}}$  is the permittivity of the oxide layer,  $t_{\text{ox}}$  is the thickness of the oxide layer,  $V_{\text{th}}$  is the threshold voltage, and  $V_g$  is the applied gate voltage.

### III. NUMERICAL RESULTS AND CONCLUSION

We assume that the monolayer  $\text{MoS}_2$  is 0.65 nm thick and 1  $\mu\text{m}$  wide. The oxide and silicon layers have thicknesses of 270 nm and 2  $\mu\text{m}$ , respectively. To calculate the local electric field inside the  $\text{MoS}_2$ , we exclude the source and drain contacts, and we treat the bottom (gate) contact as a thin film of perfectly conducting material. Figure 2 shows the output current ( $I_{ds}$ ) calculated at different drain voltages ( $V_d$ ) when gate voltage  $V_g = 0$ .

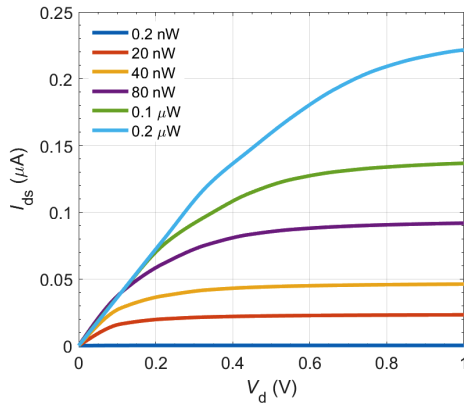


Fig. 2. Output current ( $I_{ds}$ ) at different drain voltages ( $V_d$ ) when gate voltage  $V_g = 0$ .

For quantum efficiency, we assume that the applied voltages are  $V_{ds} = -0.5 \text{ V}$  and  $V_g = 10 \text{ V}$ . The results for varying illumination wavelengths is shown in Fig. 3 with the black curve which reaches a peak at approximately 561 nm. This pattern closely mirrors the internal quantum efficiency derived from experimental simulations, denoted by the red circles [2],

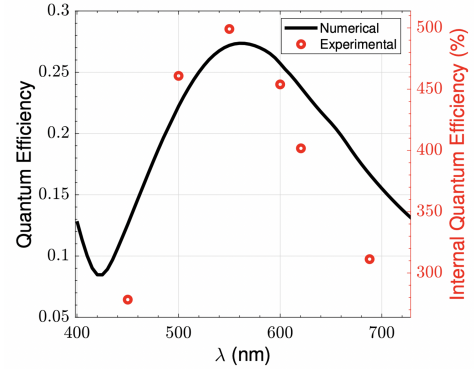


Fig. 3. Numerically obtained total quantum efficiency (left  $y$ -axis) and internal quantum efficiency (right  $y$ -axis) experimentally obtained [2].

corresponding to the right  $y$ -axis. Generally, the quantum efficiency is expected to reflect the absorption characteristics of the monolayer  $\text{MoS}_2$ . However, the influence of the  $\text{SiO}_2$  and Si layers, incorporated through the plane-wave propagation in-layered-media, introduces modifications. This observation not only validates the precision of the drift-diffusion model in characterizing the  $\text{MoS}_2$  photodetector but also underscores the importance of including the background in overall calculations.

The computation for each wavelength takes less than two minutes on a desktop computer. A more detailed analysis of the device, such as its bandwidth and how its phase noise changes with modulation frequency, will be discussed at the conference.

### REFERENCES

- [1] S. Manzeli, D. Ovchinnikov, D. Pasquier, O. V. Yazyev, and A. Kis, "2D transition metal dichalcogenides," *Nat. Rev. Mater.*, vol. 2, no. 17033, 2017.
- [2] J. Pak *et al.*, "Intrinsic optoelectronic characteristics of  $\text{MoS}_2$  phototransistors via a fully transparent van der waals heterostructure," *ACS Nano*, vol. 13, no. 8, pp. 9638–9646, 2019.
- [3] O. Lopez-Sanchez, D. Lembke, M. Kayci, A. Radenovic, and A. Kis, "Ultrasensitive photodetectors based on monolayer  $\text{MoS}_2$ ," *Nature Nanotechnology*, vol. 8, pp. 497–501, 2013.
- [4] D. Vaquero, V. Clericò, J. Salvador-Sánchez, E. Díaz, F. Domínguez-Adame, L. Chico, Y. M. Meziani, E. Diez, and J. Quereda, "Fast response photogating in monolayer  $\text{MoS}_2$  phototransistors," *Nanoscale*, vol. 13, pp. 16 156–16 163, 2021.
- [5] B. Mukherjee, F. Tseng, D. Gunlycke, K. K. Amara, G. Eda, and E. Simsek, "Complex electrical permittivity of the monolayer molybdenum disulfide ( $\text{MoS}_2$ ) in near UV and visible," *Opt. Mater. Express*, vol. 5, no. 2, pp. 447–455, Feb 2015.
- [6] K. H. Smithe, Kirby, C. D. English, S. V. Suryavanshi, and E. Pop, "High-field transport and velocity saturation in synthetic monolayer  $\text{MoS}_2$ ," *Nano Letters*, vol. 18, no. 7, pp. 4516–4522, 2018.
- [7] A. Ueda, Y. Zhang, N. Sano, H. Imamura, and Y. Iwasa, "Ambipolar device simulation based on the drift-diffusion model in ion-gated transition metal dichalcogenide transistors," *NPJ Comput. Mat.*, vol. 6, 2020.
- [8] E. Simsek, I. M. Anjum, T. F. Carruthers, C. R. Menyuk, J. C. Campbell, D. A. Tulchinsky, and K. J. Williams, "Fast evaluation of rf power spectrum of photodetectors with windowing functions," *IEEE Transactions on Electron Devices*, vol. 70, no. 7, pp. 3643–3648, 2023.
- [9] T. Korn, S. Heydrich, M. Hirmer, J. Schmutzler, and C. Schüller, "Low-temperature photocarrier dynamics in monolayer  $\text{MoS}_2$ ," *Applied Physics Letters*, vol. 99, no. 10, p. 102109, 09 2011.